Mode I Fracture Toughness Properties of *Plectocomia kerrana* Becc (Rattan) Cane

Minmin Xu, and Lili Shang *

Rattan is an important non-wood forest product, which shows a natural gradient in its structure from cane cortex to core. Toughness is its main characteristic, which is closely related to resistance to fracture. In this study, based on the principle of linear elastic fracture mechanics, the fracture toughness of *Plectocomia kerrana* Becc., was studied in two directions whose cracks were prefabricated from the cane cortex and from the cane core, respectively. The results showed that the average fracture toughness of pre-cracked from the rattan cane core was 0.476 MPa·$m^{1/2}$ measured by the SENB method. This value is much smaller than bamboo, as well as fir, Masson pine and other woods. Nominal fracture toughness of pre-cracks from cane cortex measured by flexibility method was 0.263 MPa $m^{1/2}$, which was less than the nominal fracture toughness value for pre-cracks from the core. When the rattan was bent, the crack in the rattan extended along with the prefabricated crack plane. Within the parenchymatic tissue, the crack extended transversely and changed its direction when the crack stretched into fiber sheath. The distribution density of vascular bundle was positively correlated with the fracture toughness.

DOI: 10.15376/biores.19.4.8400-8410

Keywords: Fracture toughness; Plectocomia kerrana Becc; Crack; Fiber sheath; Vascular bundle

Contact information: International Centre for Bamboo and Rattan, Beijing, China, 100102;
** Corresponding author: shangll@icbr.ac.cn*

INTRODUCTION

Rattans are spiny palm-like plants belonging to the monocotyledoneae Arecaceae. They serve as a multi-purpose plant resource with high economic utilization value (Zehui 2002). For instance, rattan cane is a good furniture making material (Ariffin *et al*. 1993; Hisham *et al*. 2014). There are 631 species, subspecies, and varieties of rattan in 11 genera in the world (Vorontsova *et al*. 2016). Of these, there are 41 species and varieties in China, which belong to 4 genera, including *Daemonorops*, *Calamus*, *Plectocomia*, and *Myrialepis* (Jiang and Wang 2018; Kang *et al.* 2018). The application of rattan is closely related to its properties. In the study of material properties, the mechanical properties are very important (Bhat *et al*. 1992; Ariffin *et al*. 1993; Hamid 2011), especially fracture toughness. Fracture is the most dangerous form of failure of materials and structures (Irwin 1970). The fracture properties of materials affect the safety, reliability, and optimal design of structure. In the initial stage of material fracture, the calculation of stress intensity factor K or G could be obtained by referring to the linear elastic mechanics formula (Shao *et al.* 2001; Mannan *et al*. 2018). Based on linear elasticity theory, the fracture of materials mainly include mode I (opening type) mode II (sliding type), mode III (shear slip type). Mode I crack development is subject to the tensile stress perpendicular to the crack surface, which opens the crack surface, and the direction of the crack extensions is perpendicular to the direction of the stress. Mode II crack formation is subjected to the shear stress parallel to the crack surface and perpendicular to the front end of the crack, so that the crack slides relatively open in the plane. Mode III crack formation is subjected to the shear stress parallel to the crack surface and parallel to the front end of the crack, which makes the crack relatively stagger, and the crack expands forward along the original direction. Among these, mode I has been found to be the most common and the most harmful (Hai *et al*. 2001; Shao *et al*. 2009; Wang *et al*. 2013; Wang *et al*. 2014; Chen *et al*. 2019). Nowadays, the fracture toughness of wood and bamboo has been subject to extensive research, especially mode I (Wang *et al*. 2014; Mannan *et al*. 2018; Chen *et al*. 2023; Zhang *et al*. 2023). Rattans as biological and natural material, which has similar cellular structure and chemical components to bamboo and wood (Liu and Zhao 2012). Thus, the fracture toughness merits study. The determination of fracture toughness mainly has included stress intensity and energy release rate method.

There has been a need for studies on the fracture toughness of rattan; therefore, in this study, the mode I fracture toughness of *Plectocomia kerrana* Becc., cane was investigated. The aims were to calculate the fracture toughness of rattan and to provide a theoretical basis for further application.

EXPERIMENTAL

Material Preparation

Plectocomia kerrana Becc., canes were collected from the nature reserve of Yingjiang County, Yunnan Province, China. Mature rattan stems with 20 to 40 mm in diameter were selected. Each of them was collected at the height of 30 cm from the ground. The leaf sheaths were cortexed off and cut into 2-m long segments. Several mature stems of rattan with an average diameter of 30 to 40 mm were selected. All the samples were prepared from the middle portions of the canes. For the testing phase, only straight canes without any visible scars, mildew, scratches, or other apparent defects were considered. The size of sample was 160 mm (length) ×20 mm (width) ×10 mm (thickness) according to the standard ASTM-E399 (2009) and ASTM E1820 (2011). Samples were kept in a conditioned room at 20±2 °C and 65±5% relative humidity until stabilization.

Pre-crack from Rattan Cane Core and Cane Cortex

The tests for fracture toughness of *Plectocomia kerrana* were carried out under three-point-bending (SENB) by using the universal mechanical testing machine (INSTRON 5582) under constant loading rate, and the crack opening displacement was measured by the COD gauge. Samples were processed into a standard three-point bending sample. The length, width, and thickness of the sample were represented by L, W, and B, respectively, and the length of the prefabricated crack was represented by a. The specimens were characterized into two categories according to the placement of the notch, notched in the rattan cane core while those notched in the rattan cane cortex (Xu *et al*. 2014). In order to simulate a naturally occurring sharp crack, the sharp cracks were notched at the center of the sample length direction, and a/W was 0.45 to 0.55. Before testing, measurements were made of the B and W of each sample at the crack section. Measurements were repeated at least three times, taking the average value, with an accuracy of 0.01 mm.

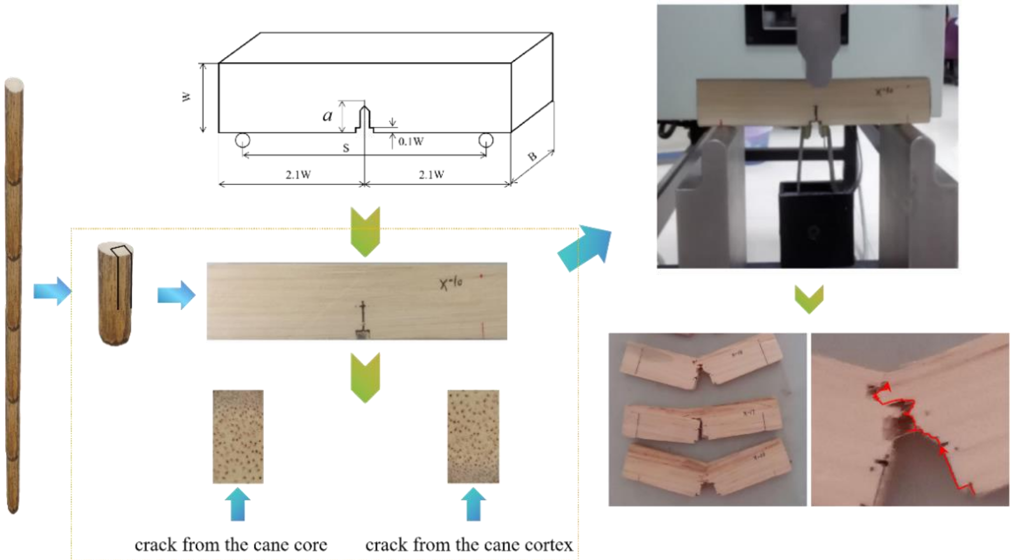

Fig. 1. Three-point bending

where L is the length of the sample, W is the width of the sample, B is the thickness of the sample, and a is the length of the prefabricated crack.

Determination of Critical Load P_Q

Nominal fracture toughness of pre-cracked from rattan cane core

The stiffness correction method was used to determine the critical load P_Q. Elastic deformation occurred in the initial stage of bending, and when the stress reached the proportional limit, the rattan entered the viscoelastic stage until the maximum failure load was reached and failure occurred. An appropriate load was applied to the SENB specimen containing the crack, so that the crack tip was according to the mode I crack type. Noting the loading state and cause of crack propagation, the load P and the opening displacement V of the COD gauge were recorded. Then the characteristic load P value on the P-V curve is determined according to the regulations, and the stiffness secant method is used to determine the load P_Q at the initial failure of the crack. The crack length a is measured, and the result is substituted into the corresponding expression to calculate the K_{IC} by fitting Eqs. 1 and 2,

$$K_{IC} = \frac{P_Q S}{HW^{3/2}} \bullet f\left(\frac{a}{W}\right) \tag{1}$$

$$f\left(\frac{a}{W}\right) = 3\sqrt{\frac{a}{W}}\,\frac{1.99-\left(\frac{a}{W}\right)\left(1-\frac{a}{W}\right)\left[2.15-3.93\frac{a}{W}+2.7\left(\frac{a}{W}\right)^2\right]}{2\left(1+2\frac{a}{W}\right)\left(1-\frac{a}{W}\right)^{3/2}} \tag{2}$$

where P_Q is the critical load at which the initial crack just appears (N), $f(a/W)$ is the geometric correction factor, S is the span between the two supports (mm), and K_{IC} is the fracture toughness (MPa •m$^{1/2}$).

Nominal fracture toughness of pre-cracked from rattan cane cortex

The P_Q value of the prefabricated cracks from the rattan cortex could no longer satisfy the theory of linear elasticity ($P_{max}/P_Q \leq 1.1$), and the calculation was carried out with reference to the ASTM E1820 standard using the energy balance point of view. According to the conversion relationship between the stress intensity factor K and the energy balance G criterion, the nominal fracture toughness was obtained by the compliance method. In the experiment, it was only necessary to measure the change rate of the compliance C of the sample with the crack length a, and then calculate G_{IC}. Then the magnitude of the stress intensity factor K could be obtained through the K-G relationship. In this paper, the dimensionless crack length ratio a/W was used to replace the crack length. This renders the results universal. Equation 5 could be replaced by Eq. 6. According to the load-displacement (P-V) curve, the compliance Ci (reciprocal of the slope of a line segment) of the corresponding specimen was calculated. The analytical expression of the compliance was obtained by fitting Eq. 6, and then K_{IC} was calculated according to Eq. 6.

$$G_{Ic} = \frac{K_{Ic}^2}{E} \tag{3}$$

$$G_{Ic} = \frac{K_I^2}{E(1-V^2)} \tag{4}$$

$$G_{IC} = \frac{P^2}{2B} \times \frac{\partial C}{\partial a} \tag{5}$$

$$G_{IC} = \frac{P^2}{2BW} \times \frac{\partial C}{\partial(\frac{a}{W})} \tag{6}$$

$$C = qe^{m(\frac{a}{W})} \tag{7}$$

where G_{IC} is the energy release rate (kJ/m^{-2}), K_{IC} is the fracture toughness (MPa •m$^{1/2}$), and C is the compliance , *i.e.*, the ratio of deformation to applied load.

Characterization

Scanning electron microscopy (SEM) (XL30 ESEM FEG; FEI Co. Hillsboro, OR, USA) was used to research the nature of the fractured surfaces of the rattan.

Vascular Bundle Measurements

The end face of the sample was intercepted, the tissue information polished to the end face of the rattan can be clearly observed by the naked eye, and then the number of vascular bundles was measured by IPP 6.0 software.

RESULTS AND DISCUSSION

K_{IC} of Pre-cracked from Rattan Cane Core

When loaded, the initial stage of rattan bending was the elastic stage, the bending load and the bending displacement were positively correlated, and the loading curve was a straight line. With the increase of the load, the rattan began to yield. Plastic deformation then occurred, and the displacement increased slowly with the increase of the bending load. When the load increased to the failure load, the rattan material showed zigzag failure, similar to the failure mode of bamboo. According to Fig. 2, it is apparent that the a/W of pre-cracked specimens from rattan cores was 0.45 to 0.55. The fracture failure curve of the rattan cane core with prefabricated cracks was consistent with the mode I fracture toughness. The K_{IC} of the pre-cracked rattan from the rattan cane core was calculated using Eq. 1. The average nominal fracture toughness of specimens with pre-cracked rattan cane cores measured by SENB was 0.476 MPa m$^{1/2}$ (from Fig. 3 and Table 1, COV=12.39%), which was much smaller than that of bamboo, fir, masson pine and other woods (Wang *et al*. 2014; Ren *et al*. 2001). It was inferred that the fracture toughness value may be related to the structure and the composition of the material.

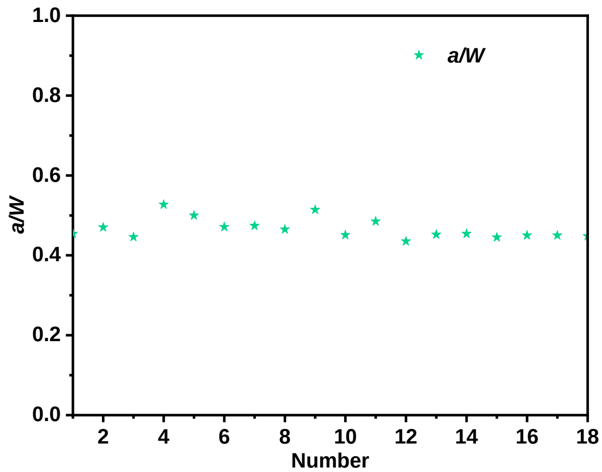

Fig. 2. Values of *a*/*W* of pre-cracked specimens from rattan cores

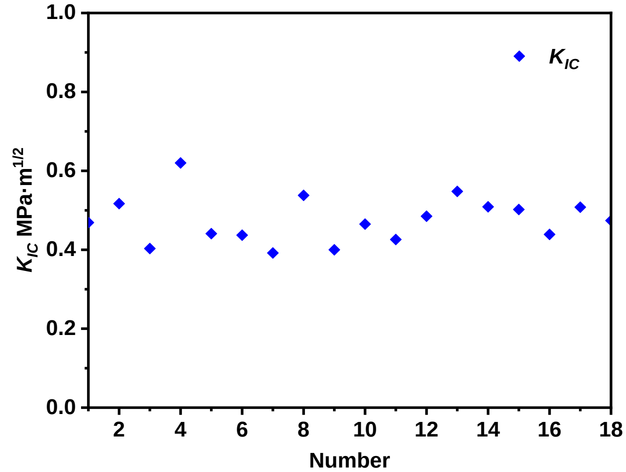

Fig. 3. K_{IC} of pre-cracked specimens from rattan cores

Table 1. Coefficient of Variation (*COV*) of Nominal Fracture Toughness Values (n, %)

Specimen Numbers	K_{IC} (Average) (MPa •m$^{1/2}$)	Standard Deviation (MPa •m$^{1/2}$)	COV %
18	0.476	0.059	12.39

K_{IC} of Pre-cracked Specimen from Rattan Cane Cortex

As most of fracture toughness test, the initial load-displacement (*P*-*V*) curve of SENB specimen with a crack was an elastic stage, the bending load and displacement were positively correlated, and the loading curve was approximately a straight line. With the increase of the load, the rattan began to yield and undergo plastic deformation. Once the crack started to expand, the bearing capacity of the specimen decreased rapidly. The *P*-*V* curve was similar to the first type of curve. The stiffness method was used to obtain the P_Q. According to the *P*-*V* curves of the crack specimens with different lengths, the flexibility corresponding to different crack lengths could be obtained *Ci* (the reciprocal of the slope of the straight-line segment) (Table 2).

Table 2. Flexibility Calibration Values of SENB Specimen

a/*W*	0.28	0.39	0.46	0.57	0.66
C_i	0.0013	0.0033	0.0058	0.0064	0.0146

By fitting the data in the table by the least squares method, the analytical expression of the test calibration curve, as shown by Eq. 8. The regression results of flexibility calibration values for SENB species were shown as Fig. 4 and the G_{IC} and K_{IC} for SENB species were shown as Fig. 5.

$$C = 0.0003e^{(5.9625*a/W)} \tag{8}$$

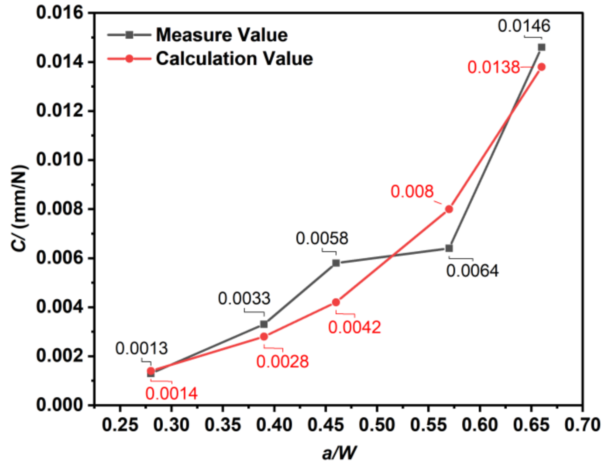

Fig. 4. Regression results of flexibility calibration values for SENB species

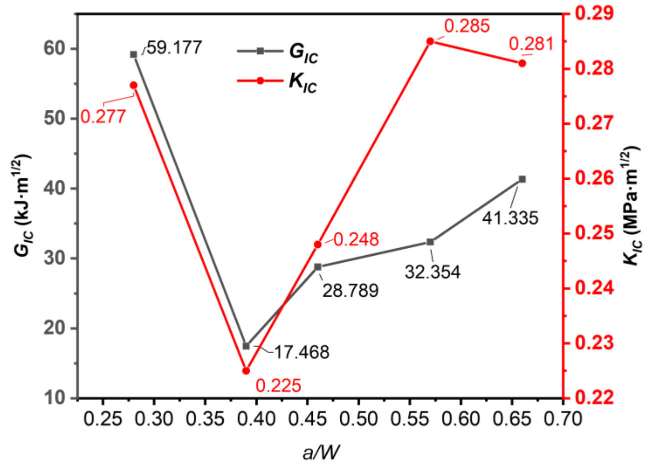

Fig. 5. G_{IC} and K_{IC} for SENB species

According to the analytical expression obtained from the fitting curve of the flexibility test (Fig. 6), the change rate of the specimen compliance with the crack length can be obtained.

$$dC/d(\frac{a}{W}) = 0.0018e^{5.9625*\frac{a}{W}} \quad (9)$$

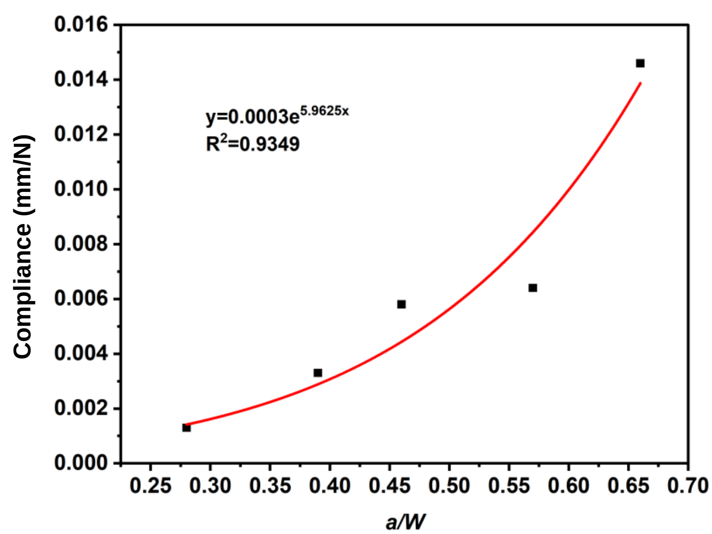

Fig. 6. (C-a/W) curve of SENB specimen

Substituting Eq. 9 into Eqs. 4 and 6, the nominal K_{IC} was obtained of pre-cracked from rattan cane cortex. The K_{IC} was 0.263 MPa m$^{1/2}$, which was smaller than that of the predicted cracks from the rattan cane core. The reason was that when there was a prefabricated crack at the rattan cane core, the force was acting at the rattan cane cortex, and the prefabricated crack from the rattan cane cortex, the force was at the rattan cane core. The mechanical properties of the rattan cane cortex were higher than those of the rattan cane core.

Fracture Failure Mode of *Plectocomia kerrana* Becc

Figure 7 shows that when the crack expanded, the fracture was basically flat; when the crack encountered the fiber bundle, the fracture would fluctuate greatly. The crack started to expand from the prefabricated crack, and generally it expanded laterally in the thin-walled basic structure area. That was along the crack prefabrication direction. When the crack encountered the interface between the fiber sheath and the thin-walled basic structure, the crack would turn to the direction of the grain. That was consistent with the previous report about bamboo (Khan *et al*. 2017; Kolawole *et al*. 2017; Yap *et al*. 2017). In the direction of the grain, the crack sometimes only propagated in one direction, and sometimes it propagated in both directions at the same time. The crack expanded to a certain length, and along with the increase of the bending stress, it expanded in the lateral direction, and so on, so that the overall propagation process of the crack was Z-shaped.

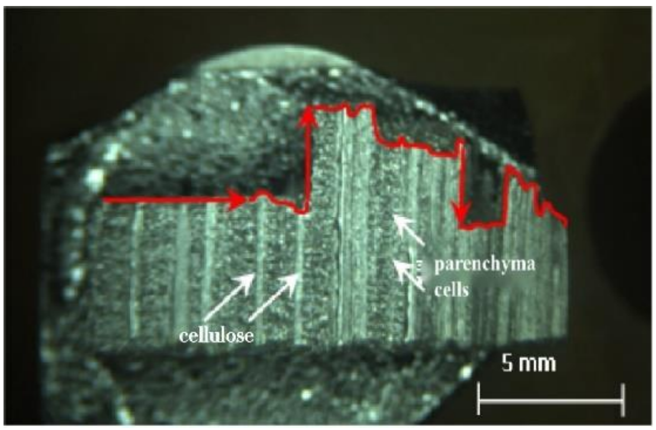

Fig. 7. Fracture side face of *Plectocomia kerrana* Becc

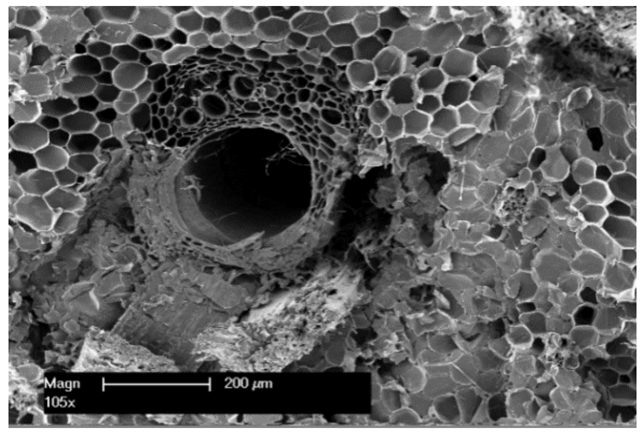

Fig. 8. Micromorphology of initial crack failure

Figure 8 shows that the crack initially propagated from the basic structure. When the crack reached the interface between the basic structure and the vascular bundle, microcracks would form on the weakly bonded interface under load, and the microcrack would follow the weak interface. Deflection occurred, which effectively prevented the original crack from expanding forward. When the load continued to rise, the interface between the fiber bundle and the basic structure would slip, and cracks would occur at the new weakly bonded interface until the fiber bundle was slowly pulled out, detached from the basic organization.

The P-V Curve of Three-point Bending Test

In the load-displacement curve of the rattan (Fig. 9), the elastic deformation of the rattan occurred first, and with the increase of bending load, the elastic-plastic deformation occurred, and the slope of the P-V curve changed from a-b to slow, as shown in the a-b section in Fig. 9. When the load reached point b, the crack expanded greatly, and the obvious force fluctuations can be observed on the P-V curve. Also the crack mainly moved along the parenchyma cells. The specimen continued to bear the load, and when the maximum value of point c was reached, the crack expanded rapidly inward, and the load decreased immediately. After the crack spread rapidly to the fiber bundle, the fiber bundle became subjected to load, so the load increased slightly to point d, and the crack expanded horizontally along the interface between the fiber bundle and the parenchyma tissue, the specimen continued to bear the load, and the elastic deformation started to store energy again. After the crack passed through the parenchyma structure, it encountered the fiber bundle, and the crack extended horizontally along the fiber interface. The load increased to point e, the fiber bundle was damaged, the load dropped greatly to point f, and the crack extended to the inner layer by layer, until finally it was completely destroyed.

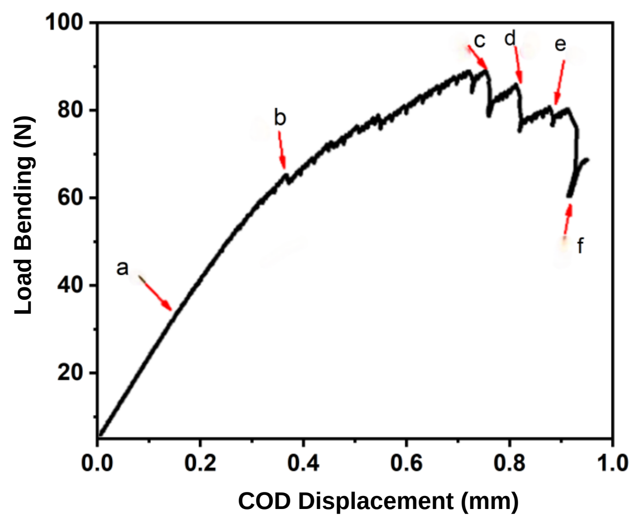

Fig. 9. The P-V curve of three-point bending test with pre-crack

The crack starts to propagate from the prefabricated crack, and then it generally expands horizontally in the basic tissue area, that is, it is along the direction of the crack prefabrication. When the crack encounters the interface between the fiber sheath and the basic tissue, the crack turns to propagate in the direction of the grain. The crack expands to a certain length, and then expands laterally with the increase of bending stress, and so on. The overall crack propagation process is Z-shaped. In the process of striated fracture, when the crack encounters the interface between the fiber sheath and the basic tissue, it will change the original propagation direction and propagate along the interface direction. The propagation path of cracks in the fiber sheath involves the coexistence of lateral expansion and longitudinal forwarding. In the basic tissue, the cracks all show a self-similar horizontal propagation pattern.

Different Vascular Bundle Content

Figure 10 shows the relationship between the fracture toughness of samples with different number of vascular bundles and the number of vascular bundles. As shown in Fig. 11, there was a linear relationship between the number of vascular bundles and the fracture toughness, and the fracture toughness of the rattan increased with the increase of the number of vascular bundles per unit area, indicating that the vascular bundle content plays an important role in the fracture toughness of the rattan. In bamboo mechanics, it is generally believed that the fiber sheath is the main load-bearing structure in the vascular bundle. Intrinsic toughening is the primary fracture toughening mechanism for bamboo. It is also the main reason why the Mode I interlaminar fracture toughness varies in different regions across the culm (Chen *et al*. 2019). The vascular bundle composition of bamboo and rattan are similar, so it can be inferred that the fiber sheath in rattan also plays a supporting role in rattan mechanics. The content of vascular bundle is actually the fiber content, and the content of vascular bundle per unit area is large, that is, the fiber content per unit area is large. The mechanism for intrinsic toughening is associated with vascular bundle, and the extent of the strained region ahead of the crack tip is also a function of the yield strength (Kolawole *et al*. 2017). The yield strength of a fiber reinforced composite generally increased with the decrease of fiber content (Ning *et al*. 2015; Taylor *et al*. 2015).

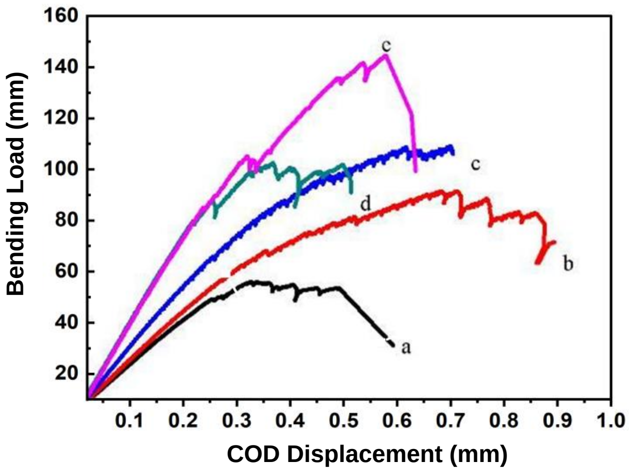

Fig. 10. The P-V curve of three-point bending with different vascular bundle content

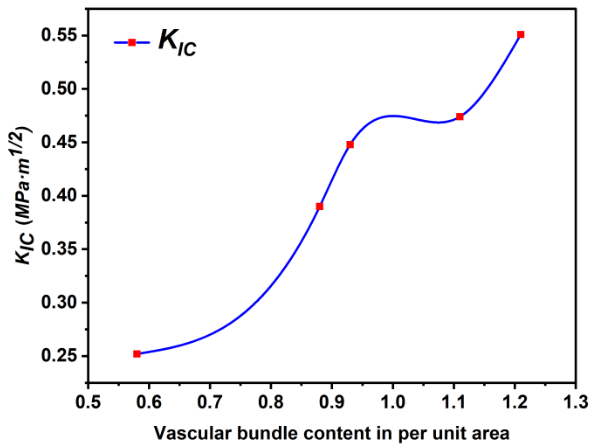

Fig. 11. The relationship between fracture toughness and vascular bundle content in per unit area

CONCLUSIONS

1. The fracture toughness of prefabricated cracks at the rattan cane core was obtained using the stress intensity factor K_{IC} criterion, and the result was 0.476 MPa·m$^{1/2}$. At the same time, the prefabricated crack from the rattan cane cortex was obtained by the energy balance G_{IC} criterion. The method used was the flexibility method, such that the flexibility expression was obtained by fitting the curve, and the G_{IC} and K_{IC} were obtained. The result was 0.263 MPa·m$^{1/2}$, which was much smaller than that from prefabricated cracks at the rattan cane core.
2. The three-point bending fracture process of *Plectocomia kerrana* Becc., was generally a step-type fracture, in which the presence of the weak interfaced in the fiber sheath and the basic parenchyma changed the propagation direction of the crack, which increased the propagation time and propagation path of the crack. The distribution density of vascular bundle was positively correlated with the fracture toughness.

ACKNOWLEDGMENTS

This work was funded by the Basic Research Fund project of the International Center for Bamboo and Rattan (2060302010408027), the Fundamental Research Funds for Research on Heat Treatment Technology of Rattan and Willow Braid for Household Use.

REFERENCES CITED

Ariffin, W. T. W., Koh, M. T., and Mustafa, M. T. (1993). “Improved rattan through phenolic resin impregnation - A preliminary study,” *Journal of Tropical Forest Science* 5(4), 485-491.

ASTM E1820 (2011). “Standard test method for measurement of fracture toughness,” ASTM International, West Conshohocken, PA, USA.

ASTM E399 (2009). “Standard test method for linear-elastic plane-strain fracture toughness of metallic materials,” ASTM International, West Conshohocken, PA, USA.

Bhat, K. M., Thulasidas, P. K., and Mohamed, C. P. (1992). “Strength properties of ten South Indian canes,” *Journal of Tropical Forest Science* 5(1), 26-34.

Chen, Q. Dai, C., Fang, C., Chen, M., Zhang, S., Liu, R., Liu, X., and Fei, B. J. (2019). “Mode I interlaminar fracture toughness behavior and mechanisms of bamboo,” *Materials and Design* 183, article 108132. DOI: 10.1016/j.matdes.2019.108132

Chen, Y., Li, H., Gao, L., Xu, W., Lorenzo, R., and Gaff, M. (2023). “A review of experimental research on the mode I fracture behavior of bamboo,” *Journal of Renewable Materials* 11(6), 2787-2808. DOI: 10.32604/jrm.2023.027634

Hai, R., Ze, J., and Zhuo, S. (2001). “Fracture toughness of plantation timber of Chinese fir and Masson pine,” *China Wood Industry* 15(01), 13-14+20.

Hamid, N. H. (2011). “Physical and mechanical properties of low quality cultivated canes modified with vinyl thermoplastics,” *The Malaysian Forester* 74(2), 123-132.

Hisham, H. N., Hale, M., and Norasikin, N. A. (2014). “Equilibrium moisture content and moisture exclusion efficiency of acetylated rattan (*Calamus manan*),” *Journal of Tropical Forest Science* 26(1), 32-40.

Irwin, G. R. (1970). “Fracture strength of relatively brittle structures and materials,” *Journal of the Franklin Institute* 290(6), 513-521. DOI: 10.1016/0016-0032(70)90234-6

Jiang, Z., and Wang, K. (2018). *Handbook of Rattan in China,* Beijing, Science Press.

Khan, Z., Yousif, B., and Islam, M. (2017). “Fracture behaviour of bamboo fiber reinforced epoxy composites,” *Composites Part B: Engineering* 116, 186-199. DOI: 10.1016/j.compositesb.2017.02.015

Kolawole, F., Olugbemi, O., Kolawole, S., Owa, A., and Ajayi, E. S. (2017). “Fracture toughness and strength of bamboo-fiber reinforced laterite as building block material,” *Universal Journal of Materials Science* 5(3), 64-72. DOI: 10.13189/ujms.2017.050302

Liu, Y., and Zhao, G. (2012). *Wood Science*, China Forestry Publishing House.

Mannan, S., Parameswaran, V., and Basu, S. (2018). “Stiffness and toughness gradation of bamboo from a damage tolerance perspective,” *International Journal of Solids and Structures* 143, 274-286. DOI: 10.1016/j.ijsolstr.2018.03.018

Ning, F., Cong, W., Qiu, J., Wei, J., and Wang, S. (2015). “Additive manufacturing of carbon fiber reinforced thermoplastic composites using fused deposition modeling,” *Composites Part B: Engineering* 80, 369-378. DOI: 10.1016/j.compositesb.2015.06.013

Ren, H. Q., Jiang, Z. H., and Shao, Z. P. (2001). “Fracture toughness of plantation timber of Chinese fir and Masson pine,” *China Wood Industry* 2001: 20013027001.

Shao, Z.-P, Fang, C.-H., and Tian, G.-L. (2009). “Mode I interlaminar fracture property of moso bamboo (*Phyllostachys pubescens*),” *Wood Science and Technology* 43, 527-

536. DOI: 10.1007/s00226-009-0265-2

Shao, Z.-P., Ren, H.-Q., and Jiang, Z.-H. (2001). “Research on the fracture toughness of wood calibrated by flexibility method,” *Forestry Science* (02), 112-116.

Taylor, D., Kinane, B., Sweeney, C., Sweetnam, D., O'Reilly, P., and Duan, K. (2015). “The biomechanics of bamboo: Investigating the role of the nodes,” *Wood Science and Technology* 49, 345-357. DOI: 10.1007/s00226-014-0694-4

Vorontsova, M.S., Clark, L.G., Dransfield, J., Govaerts, R., and Baker, W. J. (2016). *World Checklist of Bamboos and Rattans*, INBAR, Beijing, China.

Wang, F., Shao, Z., Wu, Y., and Wu, D. (2014). “The toughness contribution of bamboo node to the Mode I interlaminar fracture toughness of bamboo,” *Wood Science and Technology* 48, 1257-1268. DOI: 10.1007/s00226-013-0591-2

Wang, F., Shao, Z., and Wu, Y. (2013). “Mode II interlaminar fracture properties of Moso bamboo,” *Composites Part B: Engineering* 44(1), 242-247. DOI: 10.1016/j.compositesb.2012.05.035

Wang Kang-Lin (2018). “*Myrialepis*, a newly recorded genus in China, *Plant Science Journal*, 36(1): 11-16. DOI: 10.11913/PSJ.2095-0837.2018.10011

Xu, M., Wu, X., Liu, H., Sun, Z., Song, G., Zhang, X., and Zhao, S. (2014). “Mode I fracture toughness of tangential moso bamboo,” *BioResources* 9(2), 2026-2032. DOI: 10.15376/biores.9.2.2026-2032

Yap, C., Ming, T., Wong, K. J., and Israr, H. A. (2017). “Mechanical properties of bamboo and bamboo composites: A Review,” *J. Adv. Res. Mater. Sci.* 35(1), 7-26.

Zhang, K., Hou, Y., Lu, Y., and Wang, M. (2023). “Experimental study on the fracture toughness of bamboo scrimber,” *Materials* 16(13), article 4880. DOI: 10.3390/ma16134880

Article submitted: January 18, 2024; Peer review completed: March 9, 2024; Revised version received and accepted: June 15, 2024; Published: September 19, 2024.
DOI: 10.15376/biores.19.4.8400-8410